

# Bupropion Binds to Two Sites in the *Torpedo* Nicotinic Acetylcholine Receptor Transmembrane Domain: A Photoaffinity Labeling Study with the Bupropion Analogue [<sup>125</sup>I]-SADU-3-72

Akash Pandhare,<sup>†</sup> Ayman K. Hamouda,<sup>‡</sup> Brandon Staggs,<sup>†</sup> Shaili Aggarwal,<sup>§</sup> Phaneendra K. Duddempudi,<sup>†</sup> John R. Lever,<sup>||,⊥</sup> David J. Lapinsky,<sup>§</sup> Michaela Jansen,<sup>#</sup> Jonathan B. Cohen,<sup>‡</sup> and Michael P. Blanton<sup>\*†</sup>

<sup>†</sup>Department of Pharmacology and Neuroscience and the Center for Membrane Protein Research, School of Medicine, Texas Tech University Health Sciences Center, Lubbock, Texas 79430, United States

<sup>‡</sup>Department of Neurobiology, 220 Longwood Avenue, Harvard Medical School, Boston, Massachusetts 02115, United States

<sup>§</sup>Division of Pharmaceutical Sciences, Duquesne University, 600 Forbes Avenue, Pittsburgh, Pennsylvania 15282, United States

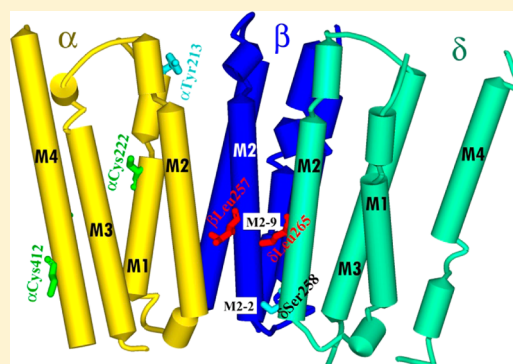
<sup>||</sup>Departments of Radiology, and Medical Pharmacology and Physiology, University of Missouri, Columbia, Missouri 65212, United States

<sup>⊥</sup>Harry S. Truman Veterans Administration Medical Center, 800 Hospital Drive, Columbia, Missouri 65201, United States

<sup>#</sup>Department of Cell Physiology and Molecular Biophysics and the Center for Membrane Protein Research, School of Medicine, Texas Tech University Health Sciences Center, Lubbock, Texas 79430, United States

## Supporting Information

**ABSTRACT:** Bupropion, a clinically used antidepressant and smoking-cessation drug, acts as a noncompetitive antagonist of nicotinic acetylcholine receptors (nAChRs). To identify its binding site(s) in nAChRs, we developed a photoreactive bupropion analogue, (±)-2-(*N*-*tert*-butylamino)-3'-[<sup>125</sup>I]-iodo-4'-azidopropiophenone (SADU-3-72). Based on inhibition of [<sup>125</sup>I]SADU-3-72 binding, SADU-3-72 binds with high affinity (IC<sub>50</sub> = 0.8 μM) to the *Torpedo* nAChR in the resting (closed channel) state and in the agonist-induced desensitized state, and bupropion binds to that site with 3-fold higher affinity in the desensitized (IC<sub>50</sub> = 1.2 μM) than in the resting state. Photolabeling of *Torpedo* nAChRs with [<sup>125</sup>I]SADU-3-72 followed by limited *in-gel* digestion of nAChR subunits with endoproteinase Glu-C established the presence of [<sup>125</sup>I]SADU-3-72 photoincorporation within nAChR subunit fragments containing M1–M2–M3 helices (αV8–20K, βV8–22/23K, and γV8–24K) or M1–M2 helices (δV8–14). Photolabeling within βV8–22/23K, γV8–24K, and δV8–14 was reduced in the desensitized state and inhibited by ion channel blockers selective for the resting (tetracaine) or desensitized (thienycyclohexylpiperidine (TCP)) state, and this pharmacologically specific photolabeling was localized to the M2-9 leucine ring (δLeu<sup>265</sup>, βLeu<sup>257</sup>) within the ion channel. In contrast, photolabeling within the αV8–20K was enhanced in the desensitized state and not inhibited by TCP but was inhibited by bupropion. This agonist-enhanced photolabeling was localized to αTyr<sup>213</sup> in αM1. These results establish the presence of two distinct bupropion binding sites within the *Torpedo* nAChR transmembrane domain: a high affinity site at the middle (M2-9) of the ion channel and a second site near the extracellular end of αM1 within a previously described halothane (general anesthetic) binding pocket.



(±)-Bupropion [(±)-2-(*tert*-butylamino)-1-(3-chlorophenyl)propan-1-one] (Figure 1) is an antidepressant agent (Well-

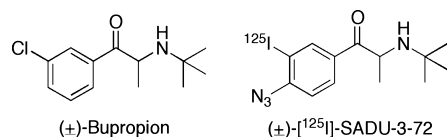


**Figure 1.** Chemical structures of bupropion and [<sup>125</sup>I]-SADU-3-72.

butrin) that is also effective in treating nicotine dependence (Zyban<sup>1</sup>). While the consensus view is that bupropion's

therapeutic efficacy as an antidepressant and a smoking cessation agent is attributable to its dual inhibition of dopamine and norepinephrine reuptake transporters, bupropion is also a noncompetitive antagonist (NCA) of several nicotinic acetylcholine receptors (nAChRs<sup>2–4</sup>). There is emerging evidence that inhibition of neuronal nAChRs, in particular α4β2 and α3β4 subtypes, may contribute to the therapeutic

**Received:** January 23, 2012

**Revised:** March 2, 2012

**Published:** March 6, 2012

benefit of bupropion as a smoking cessation agent (reviewed in ref 5).

nAChRs are members of the Cys-loop ligand-gated ion channel superfamily, which also includes  $\gamma$ -aminobutyric acid type A (GABA<sub>A</sub>) receptors, 5-hydroxytryptamine type 3 (5-HT<sub>3</sub>) receptors, glycine receptors found in vertebrates, and additional ligand-gated receptors found in invertebrates (reviewed in refs 6 and 7). Based on the three-dimensional structure of the *Torpedo* nAChR<sup>8</sup> and the available structural information regarding neuronal nAChRs (reviewed in refs 9 and 10), nAChRs are pentameric membrane proteins formed by the assembly of homologous subunits, which for the *Torpedo* nAChR has a subunit stoichiometry of  $2\alpha 1\beta 1\gamma\delta$ . Each nAChR subunit contains a large extracellular N-terminus and a bundle of four transmembrane  $\alpha$ -helices (M1–M4). The five M2 helices are arranged about a central axis orthogonal to the membrane forming the channel lumen and the M1, M3, and M4 helices form an outer ring that shield M2 from the lipid bilayer.

Pharmacological studies have shown that bupropion and its analogues noncompetitively inhibit both muscle-type (fetal human  $\alpha 1\beta 1\gamma\delta$  and *Torpedo*) and neuronal ( $\alpha 4\beta 2$ ,  $\alpha 3\beta 4$ ,  $\alpha 7$ ) nAChRs in the low to intermediate micromolar range (IC<sub>50</sub> values range from 0.4 to 60  $\mu$ M), with a rank order of potency:  $\alpha 3 \rightarrow \alpha 1-\alpha 4 \rightarrow \alpha 7$ -containing nAChRs.<sup>4,5</sup> From an analysis of bupropion effects on agonist-induced macroscopic currents for  $\alpha 1\beta 1\epsilon\delta$  (adult mouse muscle type) nAChRs expressed in HEK-293 cells, it was concluded that bupropion inhibits the receptor via two mechanisms mediated by binding to specific conformational states. Bupropion binding to the resting nAChR results in impaired channel opening (IC<sub>50</sub> 0.4  $\mu$ M), while binding to the open state results in either slow channel block or an increase in the rate of desensitization.<sup>11</sup> Radioligand competition binding experiments to *Torpedo* nAChRs further established that bupropion binds to the desensitized state with ~2-fold greater affinity than to the resting (closed) state.<sup>11</sup> While molecular docking and dynamics simulations predict that bupropion binds near the middle of the nAChR ion channel (between M2-6 and M2-13<sup>11</sup>), there has been no direct experimental identification of bupropion binding sites in any nAChR subtype.

To this end, we recently developed a photoreactive analogue of bupropion ([<sup>125</sup>I]-SADU-3-72, Figure 1<sup>12</sup>) that we use to identify and characterize the binding site(s) for bupropion in the *Torpedo* nAChR. Having established that [<sup>125</sup>I]-SADU-3-72 photolabels the *Torpedo* nAChR in a "specific" manner, that is, there is a component of labeling affected by the addition of agonist and inhibitable by bupropion or nAChR NCAs, we employed biochemical and protein chemistry approaches to identify the [<sup>125</sup>I]-SADU-3-72-labeled amino acid residues. Our results establish that bupropion does bind in the middle (M2-9) of the *Torpedo* nAChR channel in the resting and desensitized states. Further, in the desensitized state [<sup>125</sup>I]-SADU-3-72 and bupropion also bind in proximity to  $\alpha$ Tyr<sup>213</sup> in  $\alpha$ M1, a residue that resides within a halothane (general anesthetic) binding pocket.<sup>13</sup>

## ■ EXPERIMENTAL PROCEDURES

**Materials.** [<sup>125</sup>I]-SADU-3-72 (2057 Ci/mmol; Figure 1) was synthesized and radioiodinated according to the procedures outlined in.<sup>12</sup> *Torpedo californica* electric organ was obtained from Aquatic Research Consultants (San Pedro, CA). Bupropion, diisopropylfluorophosphate, bromoacetylcholine, and thienylcyclohexylpiperidine (TCP) were obtained from Sigma-Aldrich (St. Louis, MO). Trypsin (TPCK-treated) was

obtained from Worthington, *Staphylococcus aureus* glutamyl endoproteinase (Glu-C or V8 protease) was obtained from MP Biochemicals (Solon, OH), trifluoroacetic acid (TFA) was obtained from Thermo Fisher Scientific Inc. (Rockford, IL), and sodium cholate was obtained from USB Corporation (Cleveland, OH). Protease inhibitor cocktail set III and Genapol C-100 were obtained from EMD (Calbiochem; Darmstadt, Germany). Prestained low range molecular weight standards and Affigel-10 were obtained from Bio-Rad Laboratories (Hercules, CA). Synthetic lipids were obtained from Avanti Polar Lipids, Inc. (Alabaster, AL), and non-radioactive  $\alpha$ -BgTx was obtained from Biotium, Inc. (Hayward, CA). Reversed-phase HPLC columns (Brownlee Aquapore C4 column, 100  $\times$  2.1 mm, BU-300) were obtained from Perkin-Elmer Life Sciences Inc. (Boston, MA), and Centriprep-10 concentrators were obtained from Amicon Inc. (Beverly, MA).

**Preparation of Affinity-Purified *Torpedo* nAChR Membrane Vesicles.** *Torpedo californica* nAChR-rich membranes for radioligand binding studies and for affinity-purification were isolated from frozen electric organs as described previously.<sup>14</sup> *Torpedo* nAChR-rich membranes at 1 mg protein/mL were solubilized in 1% sodium cholate in vesicle dialysis buffer (VDB, 100 mM NaCl, 0.1 mM EDTA, 0.02% NaN<sub>3</sub>, 10 mM MOPS, pH 7.5) and treated with 0.1 mM diisopropylfluorophosphate after insoluble material was pelleted by centrifugation (91000g for 1 h). The nAChR was affinity-purified on a bromoacetylcholine bromide-derivatized Affi-Gel 10 column and then reconstituted into lipid vesicles composed of dioleoylphosphatidylcholine, dioleoylphosphatidic acid, and cholesterol (DOPC:DOPA:CH at a molar ratio of 3:1:1), as described.<sup>15,16</sup> The lipid to nAChR ratio was adjusted to a molar ratio of 400:1. After purification, the nAChR comprised more than 90% of the protein in the preparation based upon SDS-PAGE. Both the nAChR-rich membranes and purified nAChRs were stored at  $-80$  °C.

**Electrophysiological Recordings.** Voltage clamp electrophysiological studies were conducted using preassembled *Torpedo* nAChRs incorporated into the plasma membrane of *Xenopus* oocytes.<sup>17,18</sup> Affinity-purified *Torpedo* nAChRs reconstituted in DOPC/DOPA/CH (3:1:1 molar ratio) lipid vesicles were microinjected into oocytes (50 nL at 2.5 mg/mL protein). Following an incubation period (48 h) to allow nAChR vesicles to fuse with the plasma membrane, current recordings were performed at room temperature. Currents were recorded from individual oocytes under two-electrode voltage clamp conditions at a holding potential of  $-60$  mV. The ground electrode was connected to the bath via a 3 M KCl/agar bridge. Glass microelectrodes had a resistance of  $<2$  M $\Omega$  when filled with 3 M KCl. Data were acquired and analyzed using a TEV-200 amplifier (Dagan Instruments, Minneapolis, MN), a Digidata 1440A data interface (Molecular Devices, Sunnyvale, CA), and pClamp 10.2 software (Molecular Devices). The concentration dependence of bupropion inhibition was fit using a variable-slope sigmoidal dose response curve in Prism v5.00 (GraphPad Software, La Jolla, CA). Error bars indicate SEM acetylcholine (ACh) and bupropion were prepared as 1 M and 20 mM stock solutions, respectively, in distilled water. All solutions were made fresh from stock on the day of the experiment.

**[<sup>125</sup>I]-SADU-3-72 Competition Binding Assays.** For competition binding, *Torpedo* nAChR-rich membranes at 0.11 mg protein/mL or affinity-purified, lipid-reincorporated *Torpedo* nAChRs at 0.06 mg/mL were incubated for 5 h at room temperature with [<sup>125</sup>I]-SADU-3-72 (0.2 nM) in the

presence of  $\alpha$ -bungarotoxin ( $\alpha$ -BgTx; 1.4  $\mu$ M, 30 min preincubation) or carbamylcholine (Carb; 400  $\mu$ M) and in the presence of increasing concentrations of nonradioactive SADU-3-72, bupropion, or the NCA tetracaine (final concentrations 12.5 nM–200  $\mu$ M).  $\alpha$ -BgTx, a competitive antagonist, maintains the *Torpedo* nAChR in the closed (resting) state<sup>19</sup> while Carb stabilizes *Torpedo* nAChR in the desensitized state. The nonspecific binding was determined in the presence of 200  $\mu$ M bupropion. Bound and free [<sup>125</sup>I]-SADU-3-72 were separated by centrifugation (39000g for 1 h) and then quantified by  $\gamma$ -counting. Bound [<sup>125</sup>I]-SADU-3-72 was normalized as a percentage of specific binding (total – nonspecific binding) and fit to a simple one-site competition model using Prism v5.00 software. At the [<sup>125</sup>I]-SADU-3-72 ligand concentration used in these experiments (0.2 nM), for calculated IC<sub>50</sub> values of  $\sim$ 1  $\mu$ M, the reported IC<sub>50</sub>  $\sim$  K<sub>d</sub>.

**[<sup>125</sup>I]-SADU-3-72 Photolabeling.** For analytical labelings with [<sup>125</sup>I]-SADU-3-72, 60  $\mu$ g of affinity-purified nAChR or 125  $\mu$ g of native nAChR-rich membranes were incubated with  $\sim$ 1.5 nM [<sup>125</sup>I]-SADU-3-72 ( $\sim$ 2100 Ci/mmol) in the presence of 5  $\mu$ M  $\alpha$ -BgTx or 400  $\mu$ M Carb for 1 h at room temperature under reduced light conditions. The samples were irradiated with a 365 nm hand-held UV lamp (Spectroline EN-280 L) for 10 min at a distance of less than 1 cm and then pelleted by centrifugation (39000g for 1 h at 4 °C). Pellets were resuspended in electrophoresis sample buffer (12.5 mM Tris-HCl, 2% SDS, 8% sucrose, 1% glycerol, 0.01% bromophenol blue, pH 6.8), and the polypeptides were resolved by SDS-PAGE.

In some experiments, the NCAs tetracaine (130  $\mu$ M) or thienylcyclohexylpiperidine (TCP; 130  $\mu$ M) were added to *Torpedo* nAChR samples incubated with [<sup>125</sup>I]-SADU-3-72 in the presence of  $\alpha$ -BgTx or Carb, respectively. Tetracaine binds in the *Torpedo* nAChR channel with 30-fold higher affinity in the resting than in the desensitized state, with an established binding locus in the closed channel.<sup>20</sup> Reciprocally, TCP, a close structural analogue of phencyclidine (PCP), binds to desensitized *Torpedo* nAChR with higher affinity and with nearly identical affinity as PCP, which has an established binding locus

in the ion channel in the desensitized state.<sup>21</sup> *Torpedo* nAChR samples were incubated with [<sup>125</sup>I]-SADU-3-72 in the presence of  $\alpha$ -BgTx (1.4  $\mu$ M) or 400  $\mu$ M Carb and increasing concentrations of bupropion (12.5 nM–200  $\mu$ M).

For preparative photolabelings, 3 mg of affinity-purified, lipid-reincorporated (DOPC/DOPA/CH 3:1:1) *Torpedo* nAChRs (0.2 mg/mL) or 20 mg of native *Torpedo* nAChR-rich membranes were incubated with 7 or 15 nM [<sup>125</sup>I]-SADU-3-72 ( $\sim$ 240–700  $\mu$ Ci) under two different sets of conditions: (a) in the presence of 5  $\mu$ M  $\alpha$ -BgTx or 400  $\mu$ M Carb; (b) in the presence of 400  $\mu$ M Carb and in the absence or presence of 130  $\mu$ M TCP. These samples were then photolyzed and processed for SDS-PAGE under the same conditions as analytical labeling experiments.

**SDS–Polyacrylamide Gel Electrophoresis.** SDS-PAGE was performed according to ref 22 with separating gels comprised of 8% polyacrylamide/0.33% bis(acrylamide) (1 mm thick gels for analytical labelings; 1.5 mm thick gels for preparative labeling experiments). Following electrophoresis, gels were stained for 1 h with Coomassie Blue R-250 (0.25% (w/v) in 45% methanol, 10% acetic acid, 45% H<sub>2</sub>O) and destained (25% methanol, 10% acetic acid, 65% H<sub>2</sub>O) to visualize bands. Gels were then dried and exposed to Kodak X-OMAT LS film with an intensifying screen at –80 °C (5–24 h exposure). After autoradiography, the bands corresponding to the [<sup>125</sup>I]-SADU-3-72-labeled nAChR subunits were excised from each condition, soaked in overlay buffer (5% sucrose, 125 mM Tris-HCl, 0.1% SDS, pH 6.8) for 30 min, and transferred to the wells of a 15% acrylamide “mapping” gel.<sup>23</sup> Each gel slice was overlaid with 5  $\mu$ g (analytical labeling) or 100  $\mu$ g (preparative labeling) of *S. aureus* V8 protease in overlay buffer. After electrophoresis, the gels were stained for 1 h with Coomassie Blue R-250, destained, and either prepared for autoradiography (analytical labeling) or soaked in distilled water overnight (preparative labeling). The <sup>125</sup>I-containing bands were excised from the preparative gels, and the peptides were retrieved by passive diffusion into 25 mL of elution buffer (0.1 M NH<sub>4</sub>HCO<sub>3</sub>, 0.1% (w/v) SDS, 1%  $\beta$ -mercaptoethanol, pH 7.8) for 4 days at

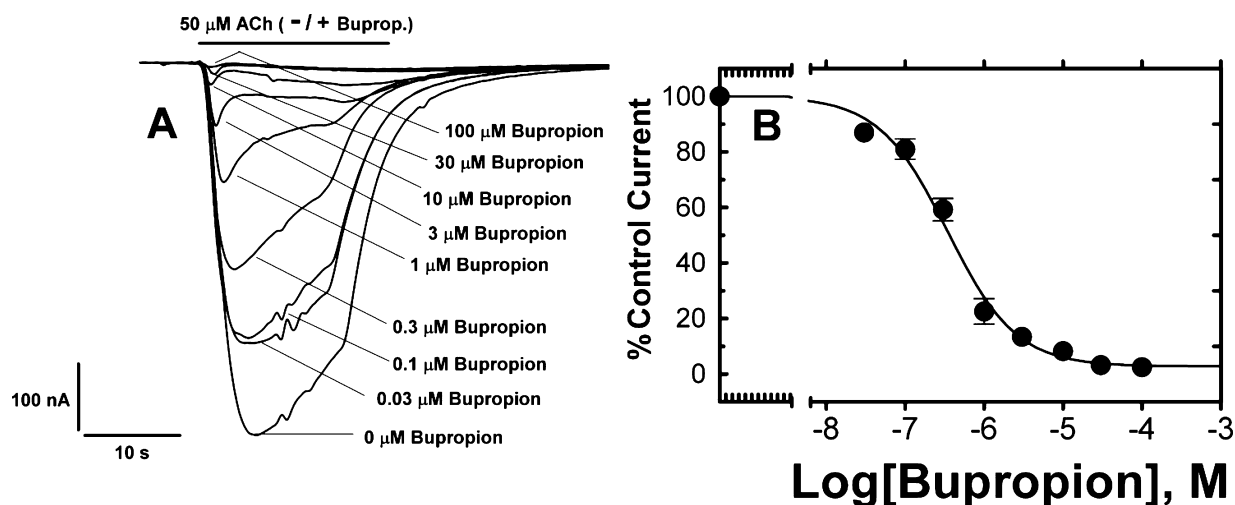


**Figure 2.** Bupropion inhibition of ACh-evoked currents of *Torpedo* AChRs microinjected into *Xenopus* oocytes. Currents elicited by ACh from affinity-purified and lipid-reconstituted (DOPC/DOPA/CH 3:1:1) *Torpedo* nAChR vesicles microinjected into *Xenopus* oocytes were measured using a standard two-electrode voltage clamp at a holding potential of –60 mV. (A) Once a stable response was observed for an EC<sub>50</sub> dose (50  $\mu$ M) of ACh, responses were measured when ACh was applied simultaneously for 20 s with increasing concentrations of bupropion (0.03–100  $\mu$ M), and in each case a representative current trace is displayed. Inhibition by bupropion was reversible since peak responses to ACh returned to control levels after exposure to 3  $\mu$ M bupropion followed by a 6 min wash (not shown). (B) Nonlinear least-squares analysis of the curves yielded an IC<sub>50</sub> = 0.34  $\pm$  0.07  $\mu$ M and nH = 0.98  $\pm$  0.14 (7 oocytes). Currents were normalized to the 50  $\mu$ M ACh response.

room temperature with gentle mixing. The eluates were filtered to remove gel pieces and then concentrated using Centriprep-10 concentrators (10 kDa cutoff, Amicon, final volume <math>\lt; 150 \mu\text{L}</math>). Samples were then either directly purified by reversed-phase HPLC or acetone precipitated (>85% acetone at  $-20^\circ\text{C}$  overnight) to remove excess SDS and then subjected to further proteolytic digestion.

**Proteolytic Digestions and Tricine SDS-PAGE.** For digestion with trypsin, acetone-precipitated subunit fragments were suspended in  $30 \mu\text{L}$  of  $0.1 \text{ M NH}_4\text{HCO}_3$ ,  $0.1\%$  SDS, pH 7.8, and then the SDS content was diluted by addition of  $113 \mu\text{L}$  of  $0.1 \text{ M NH}_4\text{HCO}_3$  and  $7.5 \mu\text{L}$  of Genapol C-100 (final concentrations:  $0.02\%$  (w/v) SDS,  $0.5\%$  Genapol C-100, pH 7.8). Trypsin ( $60 \mu\text{g}$ ) was added, and the digestion was allowed to proceed for 5 days at room temperature.

Material from each digest was then resolved on  $1.0 \text{ mm}$  thick small pore ( $16.5\%$  T/6% C) Tricine SDS-PAGE gels.<sup>24,25</sup> After Coomassie Blue R-250 staining (1 h) and destaining (3–4 h), Tricine gels were dried and exposed to film (8–12 h). The  $^{125}\text{I}$ -containing bands were excised from the Tricine gels and subjected to reversed-phase HPLC purification as indicated in the previous section.

**Reversed-Phase HPLC Purification.** HPLC was performed on a Shimadzu LC-10A binary HPLC system using a Brownlee Aquapore C<sub>4</sub> column ( $100 \times 2.1 \text{ mm}$ ). Solvent A was comprised of  $0.08\%$  trifluoroacetic acid (TFA) in water, and solvent B was comprised of  $0.05\%$  TFA in  $60\%$  acetonitrile/ $40\%$  2-propanol. A nonlinear elution gradient at  $0.2 \text{ mL/min}$  was employed (25–100% solvent B in 100 min, shown as a dotted line in the figures), and fractions were collected every 2.5 min (42 fractions/run). The elution of peptides was monitored by the absorbance at  $210 \text{ nm}$ , and the amount of  $^{125}\text{I}$  associated with each fraction was determined by  $\gamma$ -counting ( $5 \text{ min/fraction}$ ) in a Packard Cobra II  $\gamma$ -counter.

**Sequence Analysis.** Amino terminal sequence analysis of *Torpedo* nAChR subunit fragments was performed on a Applied Biosystems PROCISE 492 protein sequencer configured to utilize 1/6 of each cycle of Edman degradation for amino acid identification/quantification and collect the other 5/6 for  $^{125}\text{I}$  counting. The pooled HPLC fractions were diluted 3-fold with  $0.1\%$  TFA in distilled water (to reduce organic concentration) and loaded onto PVDF disks using Prosorb sample preparation cartridges (Applied Biosystems No. 401950). Before sequencing, filters were processed as recommended by the manufacturer. To determine the amount of the sequenced peptide, the pmol of each amino acid in a detected sequence was quantified by peak height and fit to the equation  $f(x) = I_0 R^x$ , where  $I_0$  was the initial amount of the peptide sequenced (in pmol),  $R$  was the repetitive yield, and  $f(x)$  was the pmol detected in cycle  $x$ . Ser, His, Trp, and Cys were not included in the fits due to known problems with their accurate detection/quantification. The fit was calculated in SigmaPlot 11 (SPSS) using a nonlinear least-squares method, and figures containing  $^{125}\text{I}$  release profiles (Figures 6C,D, 7B, and 8B) include this fit as a dotted line. Quantification of  $^{125}\text{I}$  incorporated into a specific residue was calculated by  $(\text{cpm}_x - \text{cpm}_{(x-1)})/5I_0R^x$ .

## RESULTS

**Functional Inhibition of *Torpedo* nAChRs by Bupropion.** To characterize bupropion as a *Torpedo* nAChR inhibitor, we employed a rather unique variant of the *Xenopus* oocyte/electrophysiology expression system introduced by the Ricardo Miledi group.<sup>17,18</sup> In this system, preassembled

*Torpedo* nAChRs are microinjected into oocytes, and following fusion of receptor containing lipid vesicles with the oocyte plasma membrane, whole-cell two-electrode voltage-clamp recordings are used to monitor receptor functionality. This system allowed us to monitor receptor functionality and bupropion effects with the same protein/receptor material that we used subsequently for bupropion binding and photoaffinity labeling experiments. In preliminary experiments, we measured ACh responses as a function of time after microinjection ( $50 \text{ nL}$ ;  $2.5 \text{ mg/mL}$  protein) of *Torpedo* nAChR-rich membranes (native nAChR) or affinity-purified and lipid reconstituted (DOPC/DOPA/CH 3:1:1) *Torpedo* nAChR (purified nAChR) that are structurally and functionally nearly indistinguishable from *Torpedo* nAChR-rich membranes.<sup>16,21,26</sup> Maximum acetylcholine (ACh) induced currents were obtained  $\sim 48 \text{ h}$  after nAChR microinjection, and the ACh dose-response curve yielded values ( $\text{EC}_{50} = 50 \mu\text{M}$ ; Hill coefficient,  $n\text{H} = 1.5$ ;  $n = 1$ ) consistent with previously published data.<sup>18</sup> Coapplication of bupropion resulted in a dose-dependent and reversible reduction in ACh-induced currents (Figure 2) with an  $\text{IC}_{50} = 0.34 \pm 0.07 \mu\text{M}$  and  $n\text{H} = 0.98 \pm 0.14$  ( $n = 7$ ). Thus,

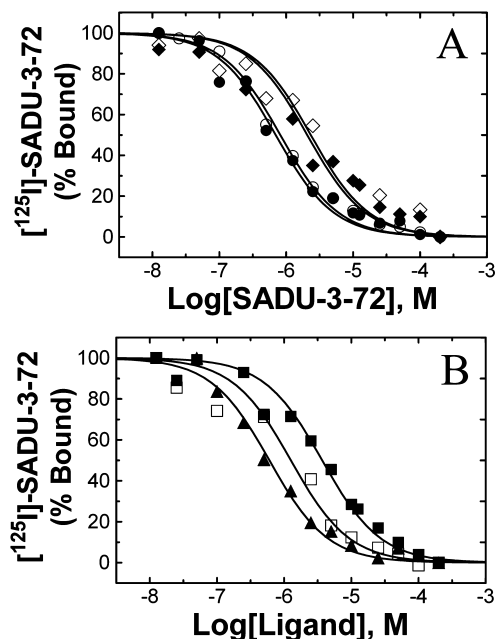


**Figure 3.** Inhibition of  $^{125}\text{I}$ -SADU-3-72 binding to *Torpedo* nAChRs by (A) SADU-3-72 and (B) bupropion or tetracaine. The equilibrium binding of  $^{125}\text{I}$ -SADU-3-72 ( $0.22 \text{ nM}$ ) to *Torpedo* nAChRs in the absence (closed symbols) or presence (open symbols) of  $400 \mu\text{M}$  Carb was determined by centrifugation. (A) SADU-3-72 inhibited binding to native nAChR-rich membranes (●, ○) with  $\text{IC}_{50}$ s of  $0.7 \pm 0.07$  (●) and  $0.8 \pm 0.08$  (○)  $\mu\text{M}$  and to affinity-purified, lipid-reconstituted nAChR with  $\text{IC}_{50}$ s of  $2.3 \pm 0.7$  (◆) and  $2.0 \pm 0.7$  (◇)  $\mu\text{M}$ . For nAChR-rich membranes, the total binding of  $^{125}\text{I}$ -SADU-3-72 was 29 078 and 26 301 cpm in the absence and presence of Carb, with 10 305 and 11 215 cpm bound nonspecifically in the presence of  $200 \mu\text{M}$  SADU-3-72. For the purified nAChR, the total binding of  $^{125}\text{I}$ -SADU-3-72 was 71 980 and 83 161 cpm in the absence and presence of Carb, with 12 211 and 12 183 cpm bound nonspecifically in the presence of  $200 \mu\text{M}$  SADU-3-72. (B) Bupropion (■, □) and tetracaine (▲) inhibited binding to *Torpedo* nAChR-rich membranes with  $\text{IC}_{50}$ s of  $3.6 \pm 0.5$  (■),  $1.2 \pm 0.3$  (□), and  $0.42 \pm 0.05$  (▲)  $\mu\text{M}$ . Nonspecific binding was determined in the presence of  $200 \mu\text{M}$  bupropion. In each case values of  $\text{IC}_{50}$  were determined by fitting the normalized specific binding to a one-site model.

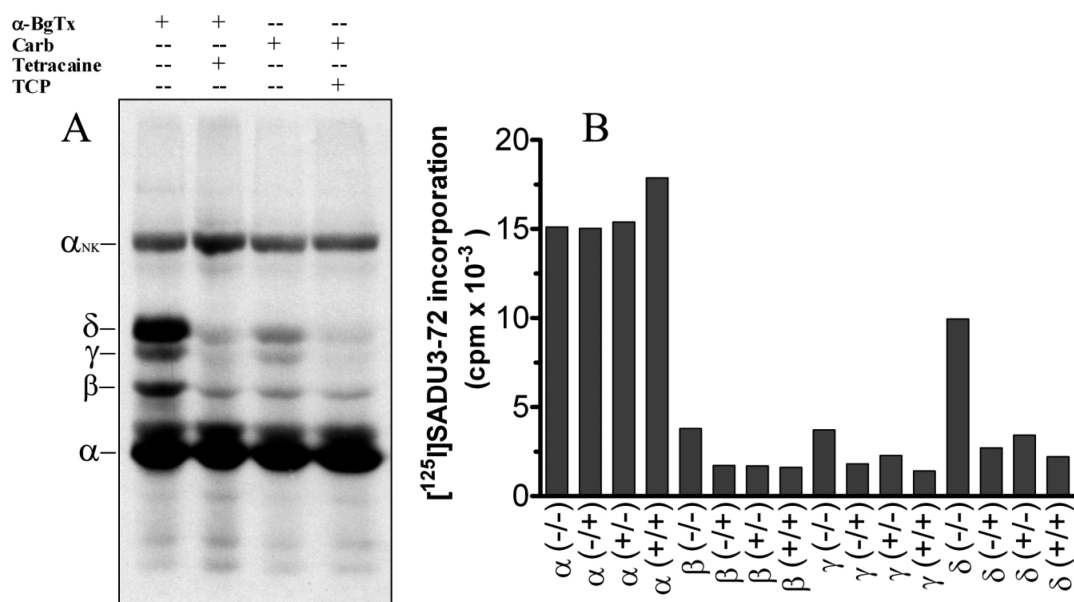


**Figure 4.** Photoincorporation of [<sup>125</sup>I]-SADU-3-72 into the *Torpedo* nAChR in the absence and presence of Carb. (A) An autoradiograph (12–24 h exposure with intensifying screen) of an 8% SDS-PAGE gel containing native *Torpedo* nAChR-rich membranes photolabeled with [<sup>125</sup>I]-SADU-3-72 in the absence (–) and/or the presence (+) of the agonist Carbamylcholine (Carb), the competitive antagonist  $\alpha$ -bungarotoxin ( $\alpha$ BgTx), the resting state-selective channel blocker tetracaine, or the desensitized state-selective channel blocker thienycyclohexylpiperidine (TCP). The migration of individual nAChR subunits and the alpha subunit of Na/K ATPase ( $\alpha_{NK}$ ) is indicated on the left. (B) [<sup>125</sup>I] cpm incorporation into each nAChR subunit for each of the labeling conditions of panel A, as determined by  $\gamma$ -counting of individual nAChR subunit bands excised from the dried gel after autoradiography ( $n = 1$ ). The notations –/–,  $\pm$ ,  $\mp$ , and +/+ indicate [<sup>125</sup>I]SADU-3-72 photolabelings in the presence of  $\alpha$ BgTx (resting state), Carb (desensitized state),  $\alpha$ BgTx and tetracaine or Carb and TCP, respectively.

bupropion inhibits *Torpedo* nAChR function with similar potency as observed for mouse  $\alpha 1\beta\epsilon\delta$  nAChRs.<sup>11</sup>

**Pharmacological Characterization of [<sup>125</sup>I]SADU-3-72 Binding to *Torpedo* nAChRs.** The effect of nonradioactive SADU-3-72 and bupropion on the equilibrium binding of [<sup>125</sup>I]SADU-3-72 to the *Torpedo* nAChR in the resting and Carb-induced desensitized states was assessed (Figure 3). SADU-3-72 inhibited [<sup>125</sup>I]SADU-3-72 binding to native nAChR ( $IC_{50}$ , 0.8  $\mu$ M) and to purified *Torpedo* nAChRs ( $IC_{50}$ , 2  $\mu$ M) in the resting or desensitized state. Bupropion had the same potencies as an inhibitor of [<sup>125</sup>I]SADU-3-72 binding to the native *Torpedo* nAChR in the desensitized state ( $IC_{50}$ , 1.2  $\pm$  0.34  $\mu$ M) or resting state ( $IC_{50}$ , 3.6  $\pm$  0.46  $\mu$ M) (Figure 3B) as reported previously for its inhibition of [<sup>3</sup>H]TCP binding.<sup>11</sup> Tetracaine, which binds in the resting state ion channel at the level of M2–9,<sup>20</sup> also fully inhibited [<sup>125</sup>I]SADU-3-72 binding (Figure 3B;  $IC_{50}$ , 0.42  $\pm$  0.05  $\mu$ M). Competition binding data were in each case well fit to a simple one-site competition model, suggesting that tetracaine, bupropion, and [<sup>125</sup>I]SADU-3-72 bind at a common site within the resting receptor.

**[<sup>125</sup>I]SADU-3-72 Photolabeling of the *Torpedo* nAChR.**

In initial photolabeling experiments we characterized photoincorporation into the *Torpedo* nAChR in the resting state (stabilized by  $\alpha$ -BgTx<sup>19</sup>) and in the desensitized state (stabilized by Carb), and we examined the effect of tetracaine or TCP on the extent of photolabeling. *Torpedo* nAChR-rich membranes or purified nAChR in lipid vesicles were photolabeled with [<sup>125</sup>I]SADU-3-72 (1.5 nM); after UV-irradiation, nAChR subunits were separated by SDS-PAGE, and photolabeling was monitored by autoradiography (Figure 4A) and by  $\gamma$ -counting of excised subunit bands (Figure 4B). A representative autoradiograph of an SDS-PAGE gel of

[<sup>125</sup>I]SADU-3-72-labeled native nAChR (Figure 4A) demonstrates photoincorporation into each nAChR subunit. In the nAChR resting state (+ $\alpha$ -BgTx), tetracaine reduced photolabeling in the  $\beta$ -,  $\gamma$ -, and  $\delta$ -subunits by 55, 51, and 73%, respectively, but by <5% in the  $\alpha$ -subunit. Compared to the nAChR resting state, [<sup>125</sup>I]SADU-3-72 photolabeling in the desensitized state (Carb +) was unchanged in the  $\alpha$ -subunit but was reduced by 50–70% in the  $\beta$ -,  $\gamma$ -, and  $\delta$ -subunits. In the nAChR desensitized state, TCP inhibited [<sup>125</sup>I]SADU-3-72 photolabeling in the  $\gamma$ - and  $\delta$ -subunits by ~35%, while photolabeling in the  $\alpha$ -subunit was increased by ~15%, and  $\beta$ -subunit labeling was unchanged. As a control, no reproducible effect on the extent of [<sup>125</sup>I]SADU-3-72 photolabeling of the  $\alpha$ -subunit of the Na,K-ATPase ( $\alpha_{NK}$  band) was observed between any of the different labeling conditions (data not shown). Qualitatively and quantitatively similar results for nAChR labeling were observed for [<sup>125</sup>I]SADU-3-72 photolabeling experiments conducted with purified *Torpedo* nAChRs (data not shown).

Bupropion also inhibited [<sup>125</sup>I]SADU-3-72 photolabeling in a concentration-dependent manner, as determined by the level of subunit photolabeling determined by SDS-PAGE. The concentration dependence of bupropion inhibition of  $\delta$  subunit photolabeling in the absence ( $IC_{50}$ , 5.5  $\pm$  0.7  $\mu$ M) and presence of Carb ( $IC_{50}$ , 2.1  $\pm$  0.7  $\mu$ M) (Supporting Information Figure S1) was similar to that seen for the inhibition of reversible [<sup>125</sup>I]SADU-3-72 binding (Figure 3B).

To further localize the site(s) of [<sup>125</sup>I]SADU-3-72 labeling within each nAChR subunit, we employed limited digestion with *S. aureus* V8 protease in a 15% acrylamide mapping gel.<sup>23</sup> Limited V8 digestion reproducibly generates a set of nonoverlapping fragments for each receptor subunit<sup>25,27–29</sup> including fragments of ~20 kDa containing the M1, M2, and M3 helices ( $\alpha$ V8-20K,  $\beta$ V8-22/23K,  $\gamma$ V8-24K) or of 14 kDa

containing the M1 and M2 helices ( $\delta$ V8-14K), and fragments of 10–14 kDa containing the M4 helix ( $\alpha$ V8-10K,  $\beta$ V8-12K, and  $\gamma$ V8-14K).

Inspection of the autoradiograph of the V8 protease digests (Figure 5A,B) and  $\gamma$  counting of the excised gel bands (Figure 5C) revealed that for nAChR in the resting state tetracaine inhibited [ $^{125}$ I]SADU-3-72 labeling within the  $\alpha$ V8-20K,  $\beta$ V8-22/23K,  $\gamma$ V8-24K, and  $\delta$ V8-14K fragments by 49, 76, 79, and 88%, respectively, which is likely to result from photolabeling in each subunit in the M2 ion channel domain. Compared to the resting state, for the nAChR desensitized state photolabeling in the  $\beta$ V8-22/23K,  $\gamma$ V8-24K, and  $\delta$ V8-14K fragments was reduced by 60, 45, and 75%, and TCP further inhibited labeling in each of these fragments. The TCP-inhibitable [ $^{125}$ I]SADU-3-72 labeling within  $\beta$ V8-22/23K,  $\gamma$ V8-24K, and  $\delta$ V8-14K predicts photolabeling of amino acids within these M2 segments. In contrast, there was an  $\sim$ 2-fold increase in photolabeling within  $\alpha$ V8-20K in the desensitized compared to resting state. This agonist-enhanced photolabeling within  $\alpha$ V8-20K was not inhibited by TCP, but bupropion did reduce the photolabeling by 70% (Figure 5C). In each subunit there was also [ $^{125}$ I]SADU-3-72 labeling that was neither affected by agonist (Carb) nor inclusion of tetracaine or TCP and that mapped to the  $\alpha$ V8-10K,  $\beta$ V8-12K,  $\beta$ V-8K, and  $\gamma$ V8-14K subunit fragments that contain the M4 helices.

**[ $^{125}$ I]SADU-3-72 Photolabeling in the M2 Ion Channel Domain.** For the *Torpedo* nAChR in the resting state, the principal site of tetracaine-inhibitable labeling resides within  $\delta$ V8-14K and  $\beta$ V8-22/23K (Figure 5). To identify the photolabeled amino acids,  $\delta$ V8-14 and  $\beta$ V8-22/23 fragments, isolated from *Torpedo* nAChRs labeled with [ $^{125}$ I]SADU-3-72 in the presence of  $\alpha$ -BgTx or Carb, were further digested with trypsin, and the digests were separated by Tricine SDS-PAGE (Supporting Information, Figure S2, panels B and C). The principal labeled fragments ( $\delta$ T-5K and  $\beta$ T-7K) isolated from the gel were further purified by reversed-phase HPLC (Figure 6A,B), and peak  $^{125}$ I cpm fractions were subjected to amino acid sequence analysis (Figure 6C,D). Sequencing revealed in each case the presence of a primary peptide beginning at the start of the M2 segment ( $\delta$ Met<sup>257</sup> and  $\beta$ Met<sup>249</sup>) and that [ $^{125}$ I]SADU-3-72-labeled homologous leucine residues ( $\delta$ Leu<sup>265</sup>, 30 cpm/pmol;  $\beta$ Leu<sup>257</sup>, 5 cpm/pmol) located nine residues from the start of the M2 segment (M2-9).

Photolabeling of  $\beta$ M2-9 and  $\delta$ M2-9 was reduced by >90% in the desensitized compared to resting state, despite the fact [ $^{125}$ I]SADU-3-72 binds with similar affinity to the nAChR in both states (Figure 3A). There was, however, TCP-inhibitable photolabeling in  $\delta$ V8-14K and  $\beta$ V8-22/23K (Figure 5). To determine whether [ $^{125}$ I]SADU-3-72 photolabeled the ion channel in the desensitized state, we carried out a preparative photolabeling of *Torpedo* nAChR in the desensitized state in the absence and presence of TCP using a higher concentration of [ $^{125}$ I]SADU-3-72. As before, the fragment beginning at  $\delta$ Met-257 was isolated from trypsin digests of  $\delta$ V8-14K by Tricine SDS-PAGE (Supporting Information, Figure S2, panel D) and reversed-phase HPLC (Figure 7A). Amino acid sequence analysis (Figure 7B) revealed the presence of a primary peptide beginning at the start of the M2 segment ( $\delta$ Met<sup>257</sup>), with a small peak of  $^{125}$ I release in cycle 9, consistent with photolabeling of  $\delta$ Leu<sup>265</sup> (M2-9, 5 cpm/pmol), and an additional peak of  $^{125}$ I release in cycle 2, which indicates photolabeling of  $\delta$ Ser<sup>258</sup> (M2-2, 3 cpm/pmol). Inclusion of 130  $\mu$ M TCP eliminated the [ $^{125}$ I]SADU-3-72 labeling of  $\delta$ Leu<sup>265</sup> (M2-9).

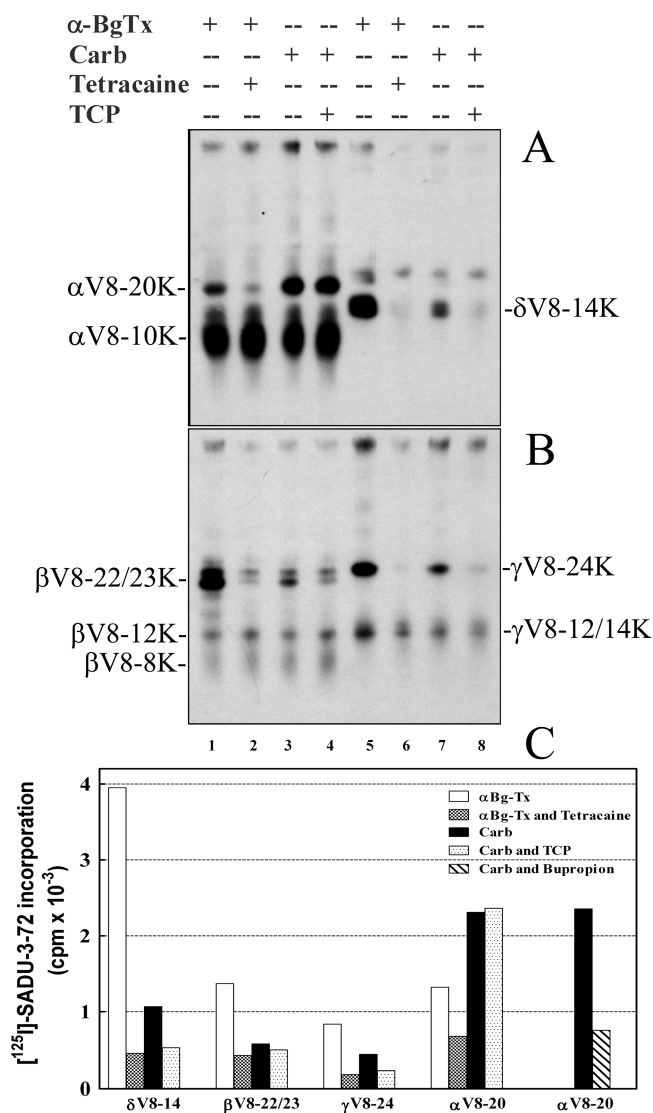


**Figure 5.** Proteolytic mapping of the sites of [ $^{125}$ I]-SADU-3-72 incorporation into AChR subunits by autoradiography (A, B) and  $\gamma$ -counting of subunit fragments (C). Native *Torpedo* nAChR-rich membranes were photolabeled with [ $^{125}$ I]-SADU-3-72 (1.5 nM) in the presence of  $\alpha$ -BgTx (resting state), – or + tetracaine (130  $\mu$ M), or Carb (desensitized state), – or + TCP (140  $\mu$ M). Subunits were resolved by SDS-PAGE on an 8% acrylamide gel, and the nAChR subunit bands were excised, transferred to the wells of a 15% mapping gel for “in gel” digestion with *S. aureus* V8 protease (see Experimental Procedures). [ $^{125}$ I]-SADU-3-72 incorporation into nAChR subunit fragments was determined by autoradiography (A,  $\alpha$ - and  $\delta$ -subunits; B,  $\beta$ - and  $\gamma$ -subunits (24 h exposure with intensifying screen)) and by  $\gamma$ -counting of excised gel bands (C). The principal [ $^{125}$ I]-SADU-3-72-labeled proteolytic fragments are shown using the nomenclature of Blanton and Cohen<sup>25</sup> (see text). (C)  $^{125}$ I cpm incorporated in  $\delta$ V8-14,  $\beta$ V8-22/23K,  $\gamma$ V8-24K, and  $\alpha$ V8-20K from the experiment of panels A and B and in  $\alpha$ V8-20K from a separate experiment for nAChRs in the presence of Carb (desensitized state) photolabeled with [ $^{125}$ I]-SADU-3-72 in the absence or presence of 130  $\mu$ M bupropion. Not included in C is the quantification by  $\gamma$ -counting of  $^{125}$ I incorporation (mean  $\pm$  SEM for the 4 conditions) in the other excised gel bands of panels A and B:  $\alpha$ V8-10K (4630  $\pm$  290 cpm),  $\beta$ V8-12K (313  $\pm$  12 cpm),  $\beta$ V-8K (326  $\pm$  18 cpm),  $\gamma$ V8-12/14K (560  $\pm$  31 cpm).

**Agonist-Dependent [ $^{125}$ I]SADU-3-72 Photolabeling within the  $\alpha$ M1.** [ $^{125}$ I]SADU-3-72 photolabeling of  $\alpha$ V8-20K was 2-fold greater in the nAChR desensitized state than in

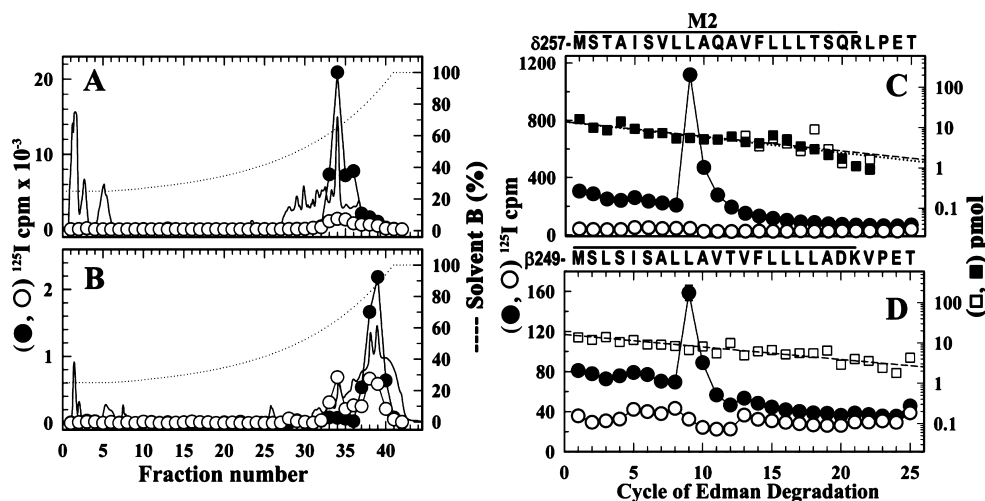


**Figure 6.** Identification of amino acids photolabeled by [<sup>125</sup>I]-SADU-3-72 in the δM2 and βM2 segments in the *Torpedo* nAChR. Affinity-purified nAChR was photolabeled with [<sup>125</sup>I]-SADU-3-72 in the presence of α-BgTx (●) or Carb (○) as detailed in the Experimental Procedures. Shown are reversed-phase HPLC fractionation (A, B) and amino acid sequence analysis (C, D) of [<sup>125</sup>I]-SADU-3-72-labeled proteolytic fragments δT-5K (A, C) and βT-7K (B, D). The elution of peptides during HPLC was monitored by absorbance at 210 nm (solid line), and <sup>125</sup>I elution was quantified by γ counting of each fraction (●, ○). (C) <sup>125</sup>I (●, ○) and PTH-amino acids (■, □) released during amino acid sequence analysis of <sup>125</sup>I peak (fractions 33–35; ●, 20 000 cpm; ○, 2000 cpm) from the HPLC purification of δT-5K. In each sample, the primary peptide detected began at δMet<sup>257</sup> (●, *I*<sub>0</sub> = 13.8 ± 2.4 pmol, *R* = 92%; ○, *I*<sub>0</sub> = 14 ± 1.5 pmol, *R* = 92%) and for the (●) sample there was a peak of <sup>125</sup>I cpm release in cycle 9 corresponding to labeling of δLeu<sup>265</sup> (30 cpm/pmol). (D) <sup>125</sup>I (●, ○) and PTH-amino acids (■, □) released during amino acid sequence analysis of <sup>125</sup>I peak (fractions 37–40; ●, 5000 cpm; ○, 1700 cpm) from the HPLC purification of βT-7K. In each sample, the primary peptide detected began at βMet<sup>249</sup> (●, *I*<sub>0</sub> = 9 ± 1 pmol, *R* = 92%; ○, *I*<sub>0</sub> = 16 ± 3 pmol, *R* = 93%) and for the (●) sample there was a peak of <sup>125</sup>I cpm release in cycle 9 corresponding to labeling of βLeu<sup>257</sup> (5 cpm/pmol).

the resting state, and photolabeling was inhibited by bupropion but not by the channel blocker TCP (Figure 5C). To further localize this Carb-enhanced, bupropion-inhibitable labeling, the αV8–20K fragments isolated from *Torpedo* nAChRs labeled with [<sup>125</sup>I]SADU-3-72 in the absence and presence of Carb were digested with trypsin, the digests separated by Tricine SDS-PAGE gel (Supporting Information, Figure S2, panel A). The principal photolabeled fragment (αT-5K) was isolated and purified by reversed-phase HPLC (Figure 8A). Amino acid sequence analysis (Figure 8B) revealed a primary peptide beginning at αIle<sup>210</sup> at the NH<sub>2</sub>-terminus of the αM1 segment. The major peak of <sup>125</sup>I release in cycle 4 indicated photolabeling of αTyr<sup>213</sup>, with labeling of this residue ~10-fold greater in the desensitized vs resting *Torpedo* nAChR (10 and 1 cpm/pmol, respectively). In addition, there was a small peak of <sup>125</sup>I release in cycle 13, consistent with [<sup>125</sup>I]SADU-3-72 labeling of αCys<sup>222</sup> at similar efficiency in the resting and desensitized states (2 cpm/pmol).

**[<sup>125</sup>I]SADU-3-72 Photolabeling in αM4.** Approximately 80% of the total [<sup>125</sup>I]SADU-3-72 photoincorporation into the α-subunit resides within the proteolytic fragment αV8-10 (Asn<sup>339</sup>-Gly<sup>437</sup>, Figure 5) with that photolabeling unaltered by inclusion of agonist or channel blockers (TCP, tetracaine). To identify the photolabeled amino acids, αV8-10K fragments, isolated from *Torpedo* nAChRs labeled with [<sup>125</sup>I]SADU-3-72 in the absence and presence of Carb, were digested with trypsin. When the digests were fractionated by reversed-phase HPLC (Supporting Information Figure S3A), all <sup>125</sup>I was recovered in a broad hydrophobic peak, which amino acid sequence analysis (Supporting Information Figure S3B) identified as a fragment beginning at αTyr<sup>401</sup> and extending through αM4, with peaks of <sup>125</sup>I release indicating [<sup>125</sup>I]SADU-3-72 labeling of αCys<sup>412</sup> and αCys<sup>418</sup>, residues previously

identified as residing at the lipid-exposed helical face of the M4 segment.<sup>8,25,30</sup>

## DISCUSSION

Bupropion became the first FDA approved non-nicotine medication (Zyban) for smoking cessation in 1997, after many years of clinical use as an antidepressant (Wellbutrin). While inhibition of presynaptic dopamine and norepinephrine transporters is believed to be the primary mechanism underlying bupropion's efficacy, there is emerging evidence that inhibition of neuronal nAChRs also contributes to its efficacy in treating nicotine dependence (reviewed in refs 4 and 5). Bupropion inhibits noncompetitively a diverse group of muscle and neuronal nAChR subtypes,<sup>4,5</sup> with a predicted binding site within the receptor's ion channel.<sup>11</sup> A novel photoreactive analogue of bupropion, (±)-2-(*N*-*tert*-butylamino)-3'-[<sup>125</sup>I]-iodo-4'-azidopropiophenone ([<sup>125</sup>I]-SADU-3-72), has been recently developed that photoincorporates into dopamine transporters and nAChRs.<sup>12</sup> In this report we used [<sup>125</sup>I]-SADU-3-72 to identify the amino acids contributing to two distinct binding sites for SADU-3-72 and bupropion in the *Torpedo* (muscle-type) nAChR transmembrane domain: the predicted binding site in the ion channel and a binding site near the extracellular end of αM1.

### Pharmacological Characterization of Bupropion and [<sup>125</sup>I]-SADU-3-72 Interactions with the *Torpedo* nAChR.

For *Torpedo* nAChRs injected into *Xenopus* oocytes, we found that bupropion inhibits reversibly ACh-induced currents with an IC<sub>50</sub> of 0.3 μM, similar to the reported IC<sub>50</sub> for bupropion inhibition of mouse muscle-type nAChR.<sup>11</sup> We also established that bupropion inhibits the reversible binding and UV-induced photoincorporation of [<sup>125</sup>I]-SADU-3-72 into the *Torpedo* nAChR with high affinity in the desensitized state (IC<sub>50</sub>'s of 1 and 2 μM), as expected for mutually exclusive binding at a

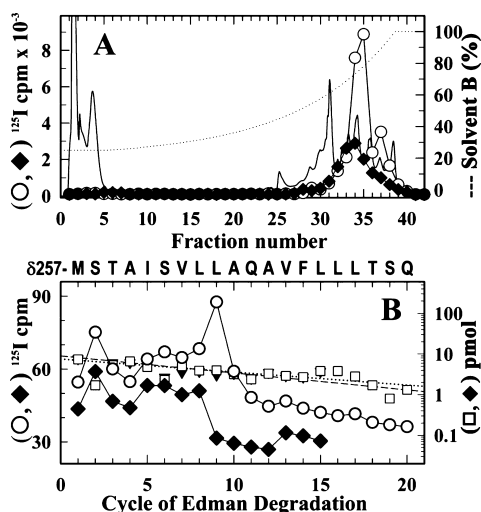


**Figure 7.** Identification of amino acids photolabeled by [<sup>125</sup>I]-SADU-3-72 in the  $\delta$ M2 segment in the desensitized *Torpedo* nAChR. nAChR-rich membranes were labeled with [<sup>125</sup>I]-SADU-3-72 in the presence of 400  $\mu$ M Carb and in the absence (O,  $\square$ ) or presence 130  $\mu$ M TCP ( $\blacklozenge$ ,  $\blacktriangledown$ ). As detailed in Experimental Procedures, the  $\delta$ -subunit was isolated from an 8% SDS-PAGE gel and digested “in-gel” with V8 protease. The labeled fragment  $\delta$ V8–14K was isolated and further digested with trypsin. The fragment  $\delta$ T5K was then isolated from a small-pore Tricine SDS-PAGE gel. Shown are reversed-phase HPLC fractionation (A) and amino acid sequence analysis (B) of [<sup>125</sup>I]-SADU-3-72-labeled proteolytic fragments  $\delta$ T-5K (A). The elution of peptides during HPLC was monitored by absorbance at 210 nm (solid line), and <sup>125</sup>I elution was quantified by  $\gamma$ -counting of each fraction (O,  $\blacklozenge$ ). (B) <sup>125</sup>I (O,  $\blacklozenge$ ) and PTH-amino acids ( $\square$ ,  $\blacktriangledown$ ) released during amino acid sequence analysis of <sup>125</sup>I peak (fractions 33–35; O, 7000 cpm;  $\blacklozenge$ , 3000 cpm) from the HPLC purification of  $\delta$ T-5K. In each sample, the primary peptide detected began at  $\delta$ Met<sup>257</sup> ( $\square$ ,  $I_0 = 9 \pm 1$  pmol,  $R = 91\%$ ;  $\blacktriangledown$ ,  $I_0 = 8 \pm 1$  pmol,  $R = 93\%$ ), and for the ( $\blacklozenge$ ) sample there were peaks of <sup>125</sup>I cpm release in cycles 2 and 9 corresponding to labeling of  $\delta$ Ser<sup>258</sup> (3 cpm/pmol) and  $\delta$ Leu<sup>265</sup> (5 cpm/pmol).

common site, and with 3-fold lower affinity in the resting state. Furthermore, tetracaine, a resting state selective ion channel blocker, inhibited the reversible binding of [<sup>125</sup>I]-SADU-3-72 ( $IC_{50}$ , 0.4  $\mu$ M) and [<sup>125</sup>I]-SADU-3-72 photoincorporation within nAChR subunit fragments containing the M2 segments (50–90% inhibition in  $\alpha$ V8-20,  $\beta$ V8-22,  $\gamma$ V8-24, and  $\delta$ V8-14), which suggested the presence of a binding site for bupropion/[<sup>125</sup>I]-SADU-3-72 within the ion channel in the nAChR resting state. For the nAChR in the desensitized state, TCP, which binds with high affinity in the ion channel in the desensitized state, inhibited [<sup>125</sup>I]-SADU-3-72 photolabeling within  $\gamma$ V8-24 and  $\delta$ V8-14, but not within  $\alpha$ V8-20, where there was agonist-enhanced photolabeling that was inhibitable by bupropion. These results indicate the presence of at least two binding sites for [<sup>125</sup>I]-SADU-3-72/bupropion in the nAChR in the desensitized state: a site within the ion channel that is inhibitable by TCP and a second site, inhibitable by bupropion, that is in proximity to amino acid(s) within  $\alpha$ M1/ $\alpha$ M2/and/or  $\alpha$ M3.

**[<sup>125</sup>I]-SADU-3-72/Bupropion Binding Site(s) in the *Torpedo* nAChR Transmembrane Domain.** The nAChR amino acids photolabeled by [<sup>125</sup>I]-SADU-3-72 are located in three different regions of the nAChR transmembrane domain (Figure 9): (i) within the ion channel, identified by photolabeling in the resting and desensitized states of the

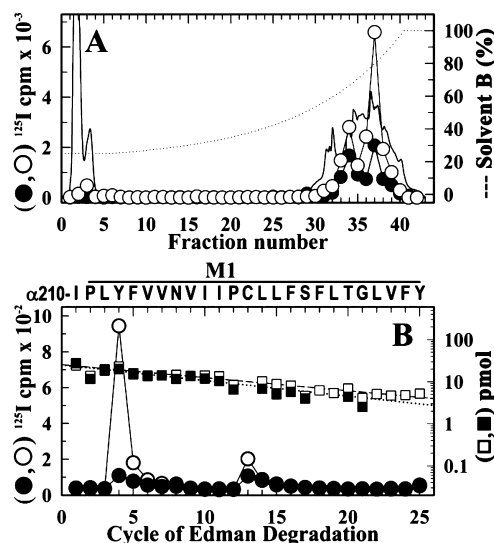


**Figure 8.** Identification of amino acids photolabeled by [<sup>125</sup>I]-SADU-3-72 in the  $\alpha$ M1 segment of the resting *Torpedo* nAChR. From the photoabeling experiment of Figure 6,  $\alpha$  subunits from affinity-purified nAChR photolabeled in the presence of  $\alpha$ -BgTx ( $\bullet$ ) or Carb (O) were digested “in-gel” with V8 protease. The labeled fragment  $\alpha$ V8-20K was then isolated and further digested with trypsin. The tryptic fragment  $\alpha$ T5K was then isolated from a small-pore Tricine SDS-PAGE gel. Shown are reversed-phase HPLC fractionation (A) and amino acid sequence analysis (B) of the [<sup>125</sup>I]-SADU-3-72-labeled  $\alpha$ T5K. (A) The elution of peptides during HPLC was monitored by absorbance at 210 nm (solid line), and <sup>125</sup>I elution was quantified by  $\gamma$  counting of each fraction ( $\bullet$ , O). (B) <sup>125</sup>I ( $\bullet$ , O) and PTH-amino acids ( $\blacksquare$ ,  $\blacktriangledown$ ) released during amino acid sequence analysis of <sup>125</sup>I peak (fractions 36–38;  $\bullet$ , 3000 cpm; O, 10 000 cpm) from the HPLC purification of  $\alpha$ T5K. In each sample, the primary peptide detected began at  $\alpha$ Leu<sup>210</sup> ( $\bullet$ ,  $I_0 = 25 \pm 2$  pmol,  $R = 92\%$ ; O,  $I_0 = 26 \pm 2$  pmol,  $R = 93\%$ ), and for both samples there were peaks of <sup>125</sup>I cpm release in cycles 4 and 13 corresponding to labeling of  $\alpha$ Tyr<sup>213</sup> ( $\bullet$ , 1 cpm/pmol; O, 10 cpm/pmol) and  $\alpha$ Cys<sup>222</sup> ( $\bullet$ , 2 cpm/pmol; O, 3 cpm/pmol).

homologous residues,  $\delta$ Leu<sup>265</sup> and  $\beta$ Leu<sup>257</sup>, at position M2-9; (ii) at the  $\alpha$ -subunit interfaces not containing the transmitter binding sites ( $\alpha^-$ ), in proximity to amino acids from the  $\gamma$ - and/or  $\beta$ -subunits, identified by the photolabeling in the desensitized state of  $\alpha$ Tyr<sup>213</sup> near the extracellular end of  $\alpha$ M1; (iii) at the lipid interface, identified by the photolabeling of  $\alpha$ Cys<sup>412</sup> and  $\alpha$ Cys<sup>418</sup> in  $\alpha$ M4 at similar efficiency in the resting and desensitized states.  $\alpha$ Cys<sup>412</sup> and  $\alpha$ Cys<sup>418</sup>, and others lying on a common strip of the  $\alpha$ M4 helix, have been photolabeled by a variety of hydrophobic probes of diverse structure and photoreactivity that partition into lipid.<sup>25,27,31,32</sup>

**[<sup>125</sup>I]-SADU-3-72/Bupropion Binding in the Ion Channel.** [<sup>125</sup>I]-SADU-3-72 photolabeled  $\beta$ M2-9 and  $\delta$ M2-9 within the ion channel at >10-fold higher efficiency in the resting state than in the desensitized state, despite the fact that [<sup>125</sup>I]-SADU-3-72 binds with similar high affinity ( $\sim 1$   $\mu$ M) in both states (Figure 3A), as does bupropion.<sup>11</sup> In this regard, [<sup>125</sup>I]-SADU-3-72 mirrors [<sup>125</sup>I]TID, a NCA that binds in the nAChR ion channel with similar high affinity in the desensitized and resting states but photolabels amino acids in the nAChR ion channel with  $\sim 10$ -fold higher efficiency in the resting state than in the desensitized state.<sup>33,34</sup> By photolabeling nAChRs in the desensitized state at a higher concentration of [<sup>125</sup>I]SADU-3-72, we also identified photolabeling of  $\delta$ Leu<sup>265</sup> (M2-9), inhibitable by TCP, and  $\delta$ Ser<sup>258</sup> (M2-2). This indicates that

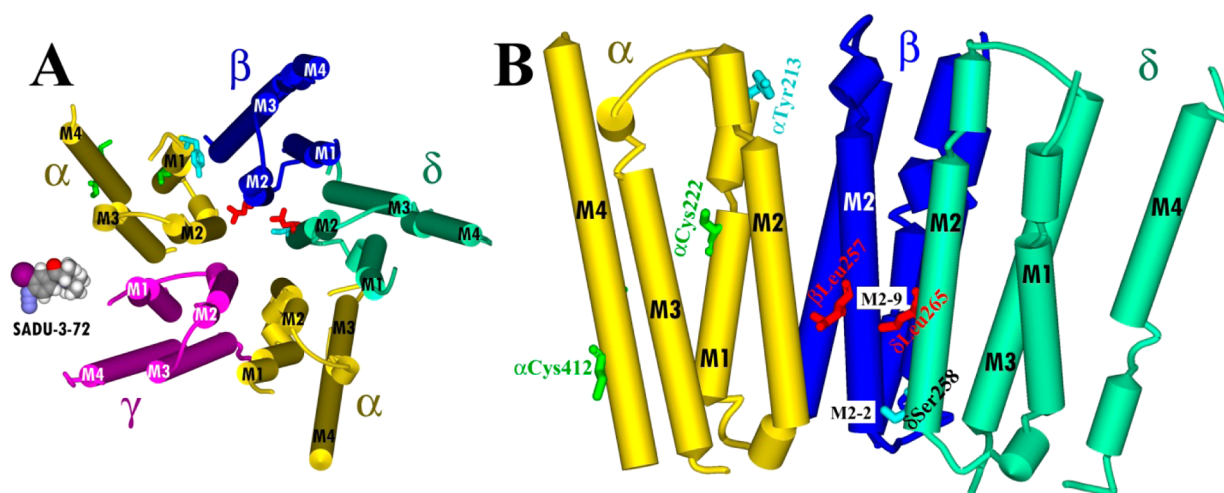


**Figure 9.** Molecular model of sites of [ $^{125}\text{I}$ ]-SADU-3-72 labeling in the *Torpedo* nAChR structure (PDB # 2BG9). Residues photolabeled by [ $^{125}\text{I}$ ]-SADU-3-72 within the transmembrane domain of the *Torpedo* nAChR. Views of the membrane-spanning helices (shown as cylinders) of the *Torpedo* nAChR structure (PDB # 2BG9): (A) looking down the channel from the base of the extracellular domain and (B) looking parallel to the membrane with 2 subunits removed for clarity, rotated  $90^\circ$  from (A). Subunits are color-coded:  $\alpha$ , yellow;  $\beta$ , blue; and  $\delta$ , green. Residues photolabeled by [ $^{125}\text{I}$ ]-SADU-3-72 are included in stick format, color-coded by domain and conformation: ion channel, resting state (red); ion channel, desensitized state (cyan); lipid-protein interface (green). A Connolly surface model of [ $^{125}\text{I}$ ]-SADU-3-72 is included in (A) for scale.

SADU3-72 and bupropion bind to the same site (M2-9) within the ion channel in the resting and desensitized states, but with a broader binding locus in the desensitized state.

**[ $^{125}\text{I}$ ]-SADU-3-72/Bupropion Binding Site in Proximity to  $\alpha\text{Tyr}^{213}$ .** The photolabeling of  $\alpha\text{Tyr}^{213}$  located near extracellular end of the  $\alpha\text{M1}$  helix was enhanced by >10-fold in the desensitized state compared to the resting state, and photolabeling of  $\alpha\text{Tyr}^{213}$  can account for the agonist-enhanced photolabeling in  $\alpha\text{V8-20}$  that was inhibitable by bupropion but not by TCP. TCP binding in the ion channel inhibited channel photolabeling by [ $^{125}\text{I}$ ]SADU-3-72, but not photolabeling of  $\alpha\text{Tyr}^{213}$ . Hence, it is unlikely that bupropion binding in the ion channel would allosterically inhibit  $\alpha\text{Tyr}^{213}$  photolabeling. Rather bupropion must inhibit competitively [ $^{125}\text{I}$ ]SADU-3-72 binding in proximity to  $\alpha\text{Tyr}^{213}$ .

$\alpha\text{Tyr}^{213}$  is photolabeled by the general anesthetic [ $^{14}\text{C}$ ]-halothane,<sup>13</sup> and amino acid substitutions at this position perturb gating, with the accessibility of  $\alpha\text{Tyr}^{213}$  Cys-substituted receptors to chemical modification increased by agonist.<sup>35,36</sup> Thus,  $\alpha\text{Tyr}^{213}$  contributes to a water-accessible, general anesthetic binding pocket located at the same interface between subunits where uncharged positive and negative nAChR allosteric modulators bind more toward the middle of the transmembrane domain.<sup>37,38</sup> The agonist-enhanced photolabeling of  $\alpha\text{Tyr}^{213}$  may be explained by the formation of SADU-3-72-accessible pocket in the vicinity of  $\alpha\text{Tyr}^{213}$  during desensitization, but further studies are required to examine the presence of this pocket and its accessibility to SADU-3-72 in resting and open states. Interestingly, we found no evidence that [ $^{125}\text{I}$ ]SADU-3-72 photolabeled amino acids in the nAChR  $\delta$  subunit helix bundle, where the uncharged inhibitor [ $^{125}\text{I}$ ]TID binds in the open and desensitized states.<sup>21,39,40</sup>

**Conclusions and Implications.** In this report, we provide a direct identification, at the amino acid level, of two distinct [ $^{125}\text{I}$ ]SADU-3-72/bupropion binding sites in the *Torpedo* nAChR. One site is at the middle of the *Torpedo* nAChR ion channel (M2-9) where SADU3-72/bupropion binds with micromolar affinity in the resting and desensitized states and is likely to contribute to their functional inhibition of the

*Torpedo* nAChR. The second site of [ $^{125}\text{I}$ ]-SADU-3-72/bupropion binding resides within a desensitized state pocket in the proximity of  $\alpha\text{Tyr}^{213}$  in  $\alpha\text{M1}$ . Though photolabeling of  $\alpha\text{Tyr}^{213}$  by [ $^{125}\text{I}$ ]SADU-3-72 provides a positive identification of this site, further studies are required to determine the affinity of SADU3-72/bupropion at this site and the functional contribution of this site to bupropion inhibition of the nAChR. Given that the channel-lining leucine residues labeled by [ $^{125}\text{I}$ ]-SADU-3-72 in the *Torpedo*  $\delta$ - and  $\beta$ -subunits are conserved in all nAChRs (as well as across the Cys loop receptor family), it is tempting to predict a common bupropion binding site at M2-9 in the ion channel in all nAChR subtypes. However, given the range of bupropion potencies for inhibition of diverse nAChR subtypes,<sup>5</sup> such an extrapolation could be an oversimplification, and the molecular determinants of bupropion binding to different nAChR ion channels may be subtype-specific. Moreover, it remains to be determined whether or not an equivalent bupropion binding site at  $\alpha\text{Tyr}^{213}$  is present in neuronal nAChRs.

## ■ ASSOCIATED CONTENT

### 📄 Supporting Information

Bupropion inhibition of [ $^{125}\text{I}$ ]-SADU-3-72 photoincorporation into the nAChR  $\delta$  subunit (Figure S1); autoradiographs of Tricine SDS-PAGE separation of tryptic digests of [ $^{125}\text{I}$ ]-SADU-3-72-labeled fragments  $\alpha\text{V8-20K}$ ,  $\beta\text{V8-22K}$ , and  $\delta\text{V8-14K}$  isolated from *Torpedo* nAChR in the resting or desensitized state (Figure S2); identification of amino acids photolabeled by [ $^{125}\text{I}$ ]-SADU-3-72 in the M4 segment of the *Torpedo* nAChR (Figure S3). This material is available free of charge via the Internet at <http://pubs.acs.org>.

## ■ AUTHOR INFORMATION

### Corresponding Author

\*Tel: (806) 743-2425; Fax: (806) 743-2744; e-mail: michael.blanton@ttuhsc.edu.

## Funding

This research was supported in part by the South Plains Foundation (M.P.B. and M.J.), by the Center for Membrane Protein Research, TTUHSC (M.P.B. and M.J.), by a Hunkele Dreaded Disease Award (D.J.L.), the Mylan School of Pharmacy at Duquesne University (D.J.L.), and by National Institutes of Health grants GM58448 (J.B.C.) and DA27081 (D.J.L.).

## Notes

The authors declare no competing financial interest.

## ACKNOWLEDGMENTS

We thank Dr. Jose-Luis Redondo (Department of Pharmacology and Neuroscience, TTUHSC) for his cell culture assistance.

## ABBREVIATIONS

nAChR, nicotinic acetylcholine receptor;  $\alpha$ -BgTx,  $\alpha$ -bungarotoxin; LGIC, ligand-gated ion channel; Carb, carbamylcholine; TCP, 1-(1-(2-thienyl)cyclohexyl) piperidine (tenocyclidine); HPLC, high-performance liquid chromatography; SDS-PAGE, sodium dodecyl sulfate polyacrylamide gel electrophoresis; TFA, trifluoroacetic acid; PTH, phenylthiohydantoin; [ $^{125}$ I]-SADU-3-72, ( $\pm$ )-2-(*N*-*tert*-butylamino)-3'-[ $^{125}$ I]-iodo-4'-azidopropiophenone hydrochloride; tricine, *N*-tris(hydroxymethyl)-methylglycine; VDB, vesicle dialysis buffer; V8 protease, *S. aureus* endoproteinase Glu-C; [ $^{125}$ I]-TID, 3-trifluoromethyl-3-(*m*-[ $^{125}$ I]-iodophenyl) diazirine.

## REFERENCES

- (1) Wilkes, S. (2008) The use of bupropion SR in cigarette smoking cessation. *Int. J. Chron. Obstruct. Pulmon. Dis.* 3, 45–53.
- (2) Fryer, J. D., and Lukas, R. J. (1999) Noncompetitive functional inhibition at diverse, human nicotinic acetylcholine receptor subtypes by bupropion, phencyclidine, and ibogaine. *J. Pharmacol. Exp. Ther.* 288, 88–92.
- (3) Slemmer, J. E., Martin, B. R., and Damaj, M. I. (2000) Bupropion is a nicotinic antagonist. *J. Pharmacol. Exp. Ther.* 295, 321–327.
- (4) Carroll, F. L., Blough, B. E., Mascarella, S. W., Navarro, H. A., Eaton, J. B., Lukas, R. J., and Damaj, M. I. (2010) Synthesis and biological evaluation of bupropion analogues as potential pharmacotherapies for smoking cessation. *J. Med. Chem.* 53, 2204–2214.
- (5) Arias, H. R. (2010) Molecular interaction of bupropion with nicotine acetylcholine receptors. *J. Pediatr. Biochem.* 1, 185–197.
- (6) Thompson, A. J., Lester, H. A., and Lummis, S. C. (2010) The structural basis of function in Cys-loop receptors. *Q. Rev. Biophys.* 43, 449–499.
- (7) Bouzat, C. (2011) New insights into the structural bases of activation of Cys-loop receptors. *J. Physiol. (Paris)*.
- (8) Unwin, N. (2005) Refined structure of the nicotinic acetylcholine receptor at 4 Å resolution. *J. Mol. Biol.* 346, 967–989.
- (9) De Biasi, M., and Dani, J. A. (2011) Reward, addiction, withdrawal to nicotine. *Annu. Rev. Neurosci.* 34, 105–130.
- (10) Dani, J. A., and Bertrand, D. (2007) Nicotinic acetylcholine receptors and nicotinic cholinergic mechanisms of the central nervous system. *Annu. Rev. Pharmacol. Toxicol.* 47, 699–729.
- (11) Arias, H. R., Gumilar, F., Rosenberg, A., Targowska-Duda, K. M., Feuerbach, D., Jozwiak, K., Moaddel, R., Wainer, I. W., and Bouzat, C. (2009) Interaction of bupropion with muscle-type nicotinic acetylcholine receptors in different conformational states. *Biochemistry* 48, 4506–4518.
- (12) Lapinsky, D. J., Aggarwal, S., Nolan, T. L., Surratt, C. K., Lever, J. R., Acharya, R., Vaughan, R. A., Pandhare, A., and Blanton, M. P. (2012) ( $\pm$ )-2-(*N*-*tert*-Butylamino)-3'-[ $^{125}$ I]-iodo-4'-azidopropiophenone: A dopamine transporter and nicotinic acetylcholine receptor

photoaffinity ligand based on bupropion (Wellbutrin, Zyban). *Bioorg. Med. Chem. Lett.* 22, 523–526.

(13) Chiara, D. C., Dangott, L. J., Eckenhoff, R. G., and Cohen, J. B. (2003) Identification of nicotinic acetylcholine receptor amino acids photolabeled by the volatile anesthetic halothane. *Biochemistry* 42, 13457–13467.

(14) Pedersen, S. E., Dreyer, E. B., and Cohen, J. B. (1986) Location of ligand-binding sites on the nicotinic acetylcholine receptor alpha-subunit. *J. Biol. Chem.* 261, 13735–13743.

(15) Fong, T. M., and McNamee, M. G. (1986) Correlation between acetylcholine receptor function and structural properties of membranes. *Biochemistry* 25, 830–840.

(16) Hamouda, A. K., Sanghvi, M., Sauls, D., Machu, T. K., and Blanton, M. P. (2006) Assessing the lipid requirements of the Torpedo californica nicotinic acetylcholine receptor. *Biochemistry* 45, 4327–4337.

(17) Marsal, J., Tigyi, G., and Miledi, R. (1995) Incorporation of acetylcholine receptors and Cl<sup>-</sup> channels in *Xenopus* oocytes injected with Torpedo electroplaque membranes. *Proc. Natl. Acad. Sci. U. S. A.* 92, 5224–5228.

(18) Morales, A., Aleu, J., Ivorra, I., Ferragut, J. A., Gonzalez-Ros, J. M., and Miledi, R. (1995) Incorporation of reconstituted acetylcholine receptors from Torpedo into the *Xenopus* oocyte membrane. *Proc. Natl. Acad. Sci. U. S. A.* 92, 8468–8472.

(19) Moore, M. A., and McCarthy, M. P. (1995) Snake venom toxins, unlike smaller antagonists, appear to stabilize a resting state conformation of the nicotinic acetylcholine receptor. *Biochim. Biophys. Acta* 1235, 336–342.

(20) Gallagher, M. J., and Cohen, J. B. (1999) Identification of amino acids of the torpedo nicotinic acetylcholine receptor contributing to the binding site for the noncompetitive antagonist [(3)H]tetraacine. *Mol. Pharmacol.* 56, 300–307.

(21) Hamouda, A. K., Chiara, D. C., Blanton, M. P., and Cohen, J. B. (2008) Probing the structure of the affinity-purified and lipid-reconstituted torpedo nicotinic acetylcholine receptor. *Biochemistry* 47, 12787–12794.

(22) Laemmli, U. K. (1970) Cleavage of structural proteins during the assembly of the head of bacteriophage T4. *Nature* 227, 680–685.

(23) Cleveland, D. W., Fischer, S. G., Kirschner, M. W., and Laemmli, U. K. (1977) Peptide mapping by limited proteolysis in sodium dodecyl sulfate and analysis by gel electrophoresis. *J. Biol. Chem.* 252, 1102–1106.

(24) Schagger, H., and von Jagow, G. (1987) Tricine-sodium dodecyl sulfate-polyacrylamide gel electrophoresis for the separation of proteins in the range from 1 to 100 kDa. *Anal. Biochem.* 166, 368–379.

(25) Blanton, M. P., and Cohen, J. B. (1994) Identifying the lipid-protein interface of the Torpedo nicotinic acetylcholine receptor: secondary structure implications. *Biochemistry* 33, 2859–2872.

(26) Baenziger, J. E., Morris, M. L., Darsaut, T. E., and Ryan, S. E. (2000) Effect of membrane lipid composition on the conformational equilibria of the nicotinic acetylcholine receptor. *J. Biol. Chem.* 275, 777–784.

(27) Blanton, M. P., Dangott, L. J., Raja, S. K., Lala, A. K., and Cohen, J. B. (1998) Probing the structure of the nicotinic acetylcholine receptor ion channel with the uncharged photoactivable compound -3H-diazofluorene. *J. Biol. Chem.* 273, 8659–8668.

(28) Blanton, M. P., McCardy, E. A., Huggins, A., and Parikh, D. (1998) Probing the structure of the nicotinic acetylcholine receptor with the hydrophobic photoreactive probes [125I]TID-BE and [125I]TIDPC/16. *Biochemistry* 37, 14545–14555.

(29) Blanton, M. P., Li, Y. M., Stimson, E. R., Maggio, J. E., and Cohen, J. B. (1994) Agonist-induced photoincorporation of a p-benzoylphenylalanine derivative of substance P into membrane-spanning region 2 of the Torpedo nicotinic acetylcholine receptor delta subunit. *Mol. Pharmacol.* 46, 1048–1055.

(30) Miyazawa, A., Fujiyoshi, Y., and Unwin, N. (2003) Structure and gating mechanism of the acetylcholine receptor pore. *Nature* 423, 949–955.

(31) Blanton, M. P., Xie, Y., Dangott, L. J., and Cohen, J. B. (1999) The steroid promegestone is a noncompetitive antagonist of the Torpedo nicotinic acetylcholine receptor that interacts with the lipid-protein interface. *Mol. Pharmacol.* 55, 269–278.

(32) Garcia, G. III, Chiara, D. C., Nirthanan, S., Hamouda, A. K., Stewart, D. S., and Cohen, J. B. (2007) [<sup>3</sup>H]Benzophenone photolabeling identifies state-dependent changes in nicotinic acetylcholine receptor structure. *Biochemistry* 46, 10296–10307.

(33) White, B. H., Howard, S., Cohen, S. G., and Cohen, J. B. (1991) The hydrophobic photoreagent 3-(trifluoromethyl)-3-m-([<sup>125</sup>I]iodophenyl) diazirine is a novel noncompetitive antagonist of the nicotinic acetylcholine receptor. *J. Biol. Chem.* 266, 21595–21607.

(34) White, B. H., and Cohen, J. B. (1992) Agonist-induced changes in the structure of the acetylcholine receptor M2 regions revealed by photoincorporation of an uncharged nicotinic noncompetitive antagonist. *J. Biol. Chem.* 267, 15770–15783.

(35) Akabas, M. H., and Karlin, A. (1995) Identification of acetylcholine receptor channel-lining residues in the M1 segment of the alpha-subunit. *Biochemistry* 34, 12496–12500.

(36) Yu, Y., Shi, L., and Karlin, A. (2003) Structural effects of quinacrine binding in the open channel of the acetylcholine receptor. *Proc. Natl. Acad. Sci. U. S. A.* 100, 3907–3912.

(37) Nirthanan, S., Garcia, G. III, Chiara, D. C., Husain, S. S., and Cohen, J. B. (2008) Identification of binding sites in the nicotinic acetylcholine receptor for TDBzl-etomidate, a photoreactive positive allosteric effector. *J. Biol. Chem.* 283, 22051–22062.

(38) Hamouda, A. K., Stewart, D. S., Husain, S. S., and Cohen, J. B. (2011) Multiple transmembrane binding sites for p-trifluoromethyl-diaziriny-etomidate, a photoreactive Torpedo nicotinic acetylcholine receptor allosteric inhibitor. *J. Biol. Chem.* 286, 20466–20477.

(39) Arevalo, E., Chiara, D. C., Forman, S. A., Cohen, J. B., and Miller, K. W. (2005) Gating-enhanced accessibility of hydrophobic sites within the transmembrane region of the nicotinic acetylcholine receptor's  $\delta$ -subunit. A time-resolved photolabeling study. *J. Biol. Chem.* 280, 13631–13640.

(40) Yamodo, I. H., Chiara, D. C., Cohen, J. B., and Miller, K. W. (2010) Conformational changes in the nicotinic acetylcholine receptor during gating and desensitization. *Biochemistry* 49, 156–165.